Supporting Information for

Reduction of Aqueous CO_2 to 1-Propanol at MoS_2 Electrodes

Sonja A. Francis[†,a,1], Jesus M. Velazquez[†a,,2], Ivonne M. Ferrer[a], Daniel A. Torelli[a], Dan Guevarra[a], Matthew T. McDowell[a,3], Ke Sun[a], Xinghao Zhao[b], Fadl H. Saadi[b], Jimmy John[a], Matthias Richter[a], Forrest P. Hyler[c], Kimberly M. Papadantonakis[a], Bruce S. Brunschwig[d], Nathan S. Lewis[*,a,d]

[a]Division of Chemistry and Chemical Engineering, [b]Division of Engineering and Applied Sciences, and [d]Beckman Institute, California Institute of Technology, Pasadena, California 91125, United States
[c]Department of Chemistry, University of California, Davis, California 95616, United States

Corresponding Author

* Email: nslewis@caltech.edu.

Present Addresses

[1] Department of Chemistry, Princeton University.
[2] Department of Chemistry, University of California, Davis.
[3] G. W. Woodruff School of Mechanical Engineering and School of Materials Science and Engineering, Georgia Institute of Technology.

Author contributions

[†] These authors contributed equally to this work.

Table of Contents

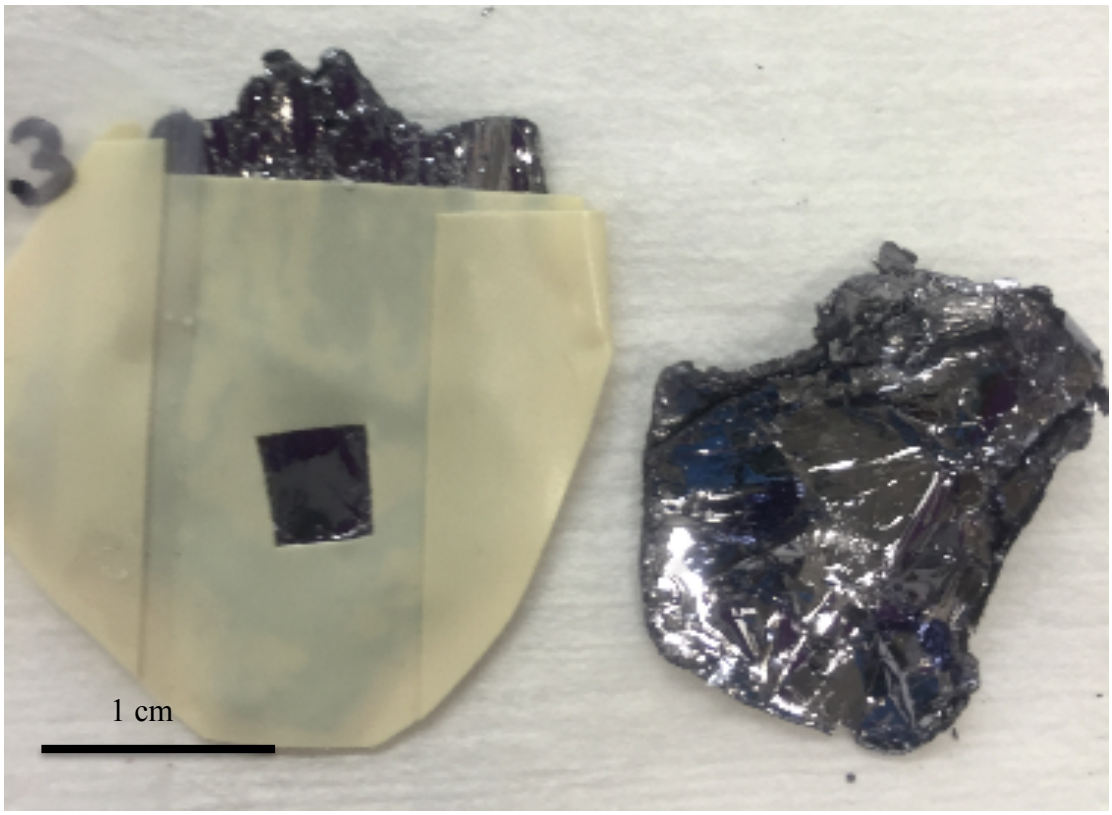

Figure S1. Photograph of a MoS_2 single crystal with electroplating tape applied to mask edge-dense areas (left) and an un-masked crystal with large amounts of edges (right).

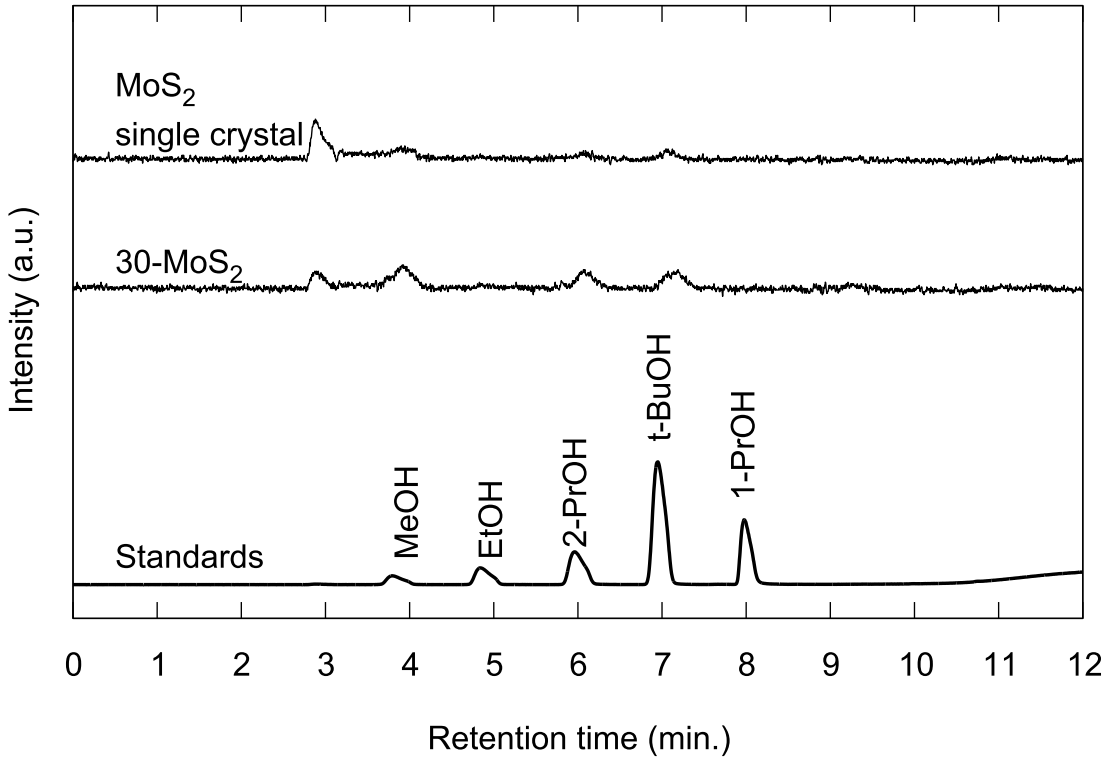

Figure S2. Representative GC-HS chromatograms of a liquid aliquot removed from the electrochemical cell after electrolysis at -0.59 V vs. RHE in 0.10 M Na_2CO_3 acidified to pH 6.8 with 1 atm CO_2 on (top) MoS_2 single crystals and (center) 30-MoS_2 showing production of alcohols, compared to standard solutions (Bottom). Note that standards of acetone (not shown) have similar retention times to 2-propanol.

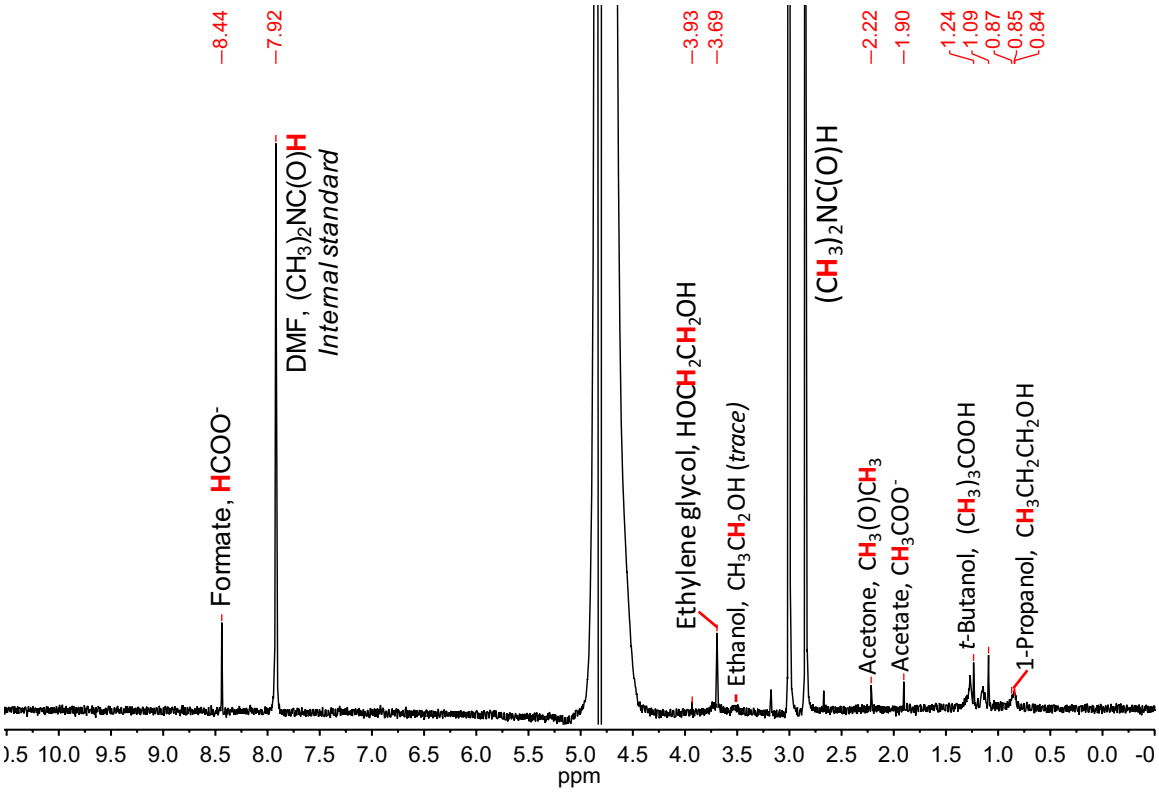

Figure S3. Representative NMR spectrum for electrolysis at -0.59 V vs. RHE for a single crystal of MoS_2 in 0.10 M Na_2CO_3 acidified to pH 6.8 with 1 atm CO_2. Peak chemical shifts are identified in Table S1.

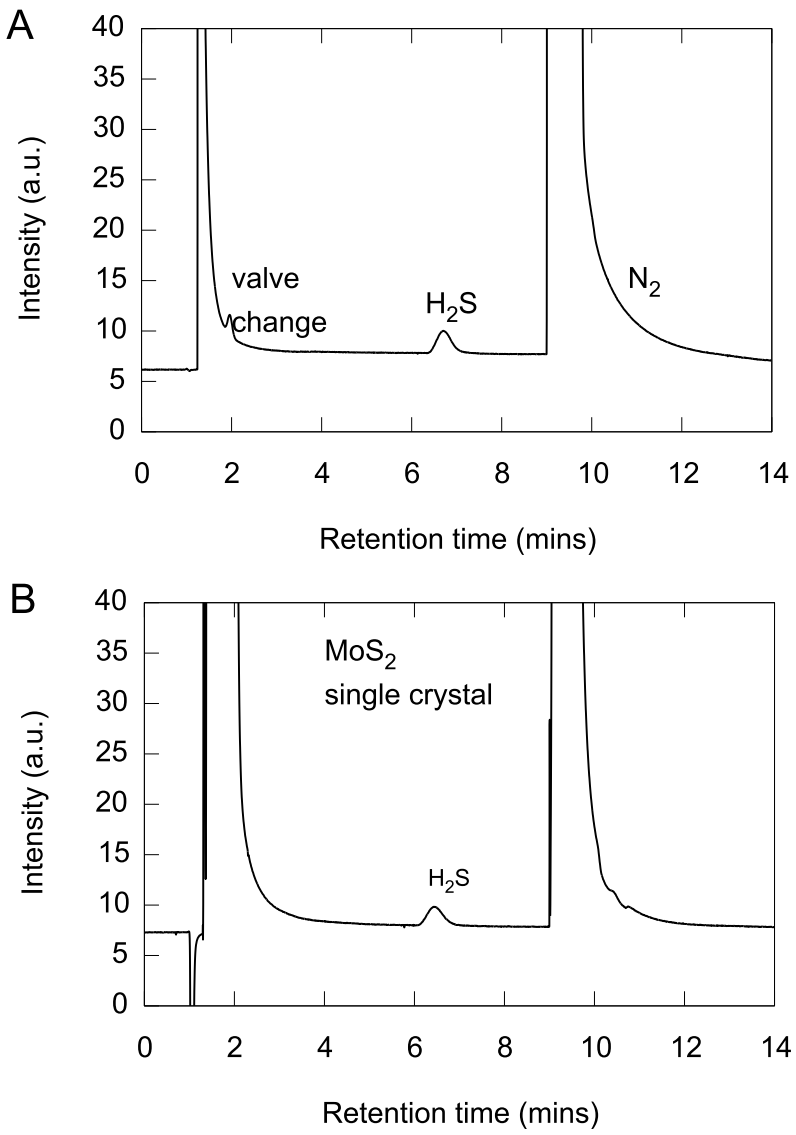

Figure S4. Representative GC-TCD chromatograms showing the retention time for (A) a H_2S standard made in situ from FeS and HCl in inert nitrogen atmosphere, and (B) H_2S produced during bulk electrolysis in 0.10 M Na_2CO_3 acidified to pH 6.8 with 1 atm CO_2 at -0.59 V vs. RHE at a MoS_2 single crystal terrace.

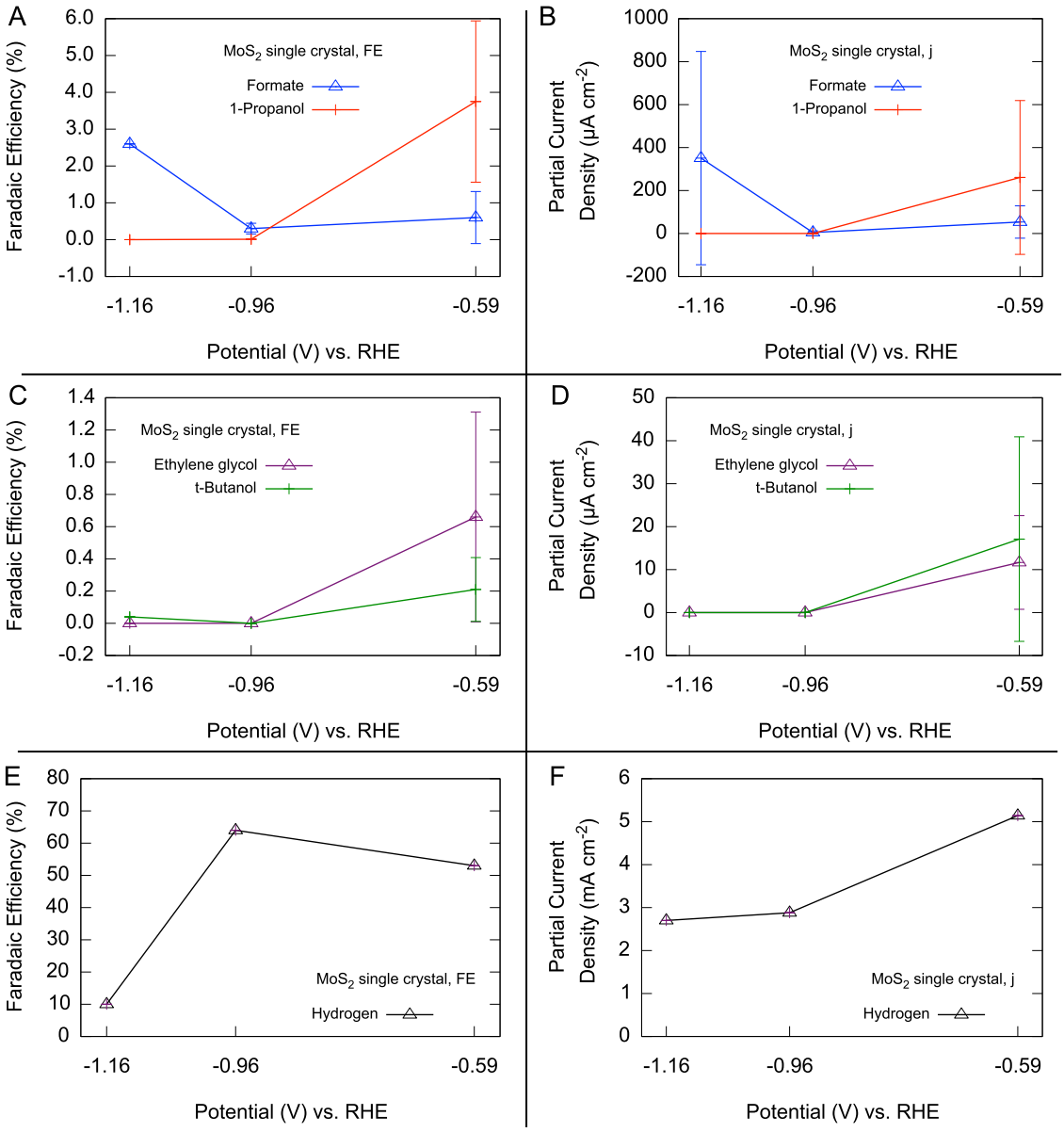

Figure S5. Potential-dependent Faradaic efficiencies (left) and partial current densities (right) for major (A,B), and minor CO_2R products (C,D), and proton reduction (E,F) on MoS_2 single crystals with masked edge sites. The electrolyte was 0.10 M Na_2CO_3 (aq) acidified to pH 6.8 with 1 atm CO_2. Standard deviations are indicated for CO_2R products.

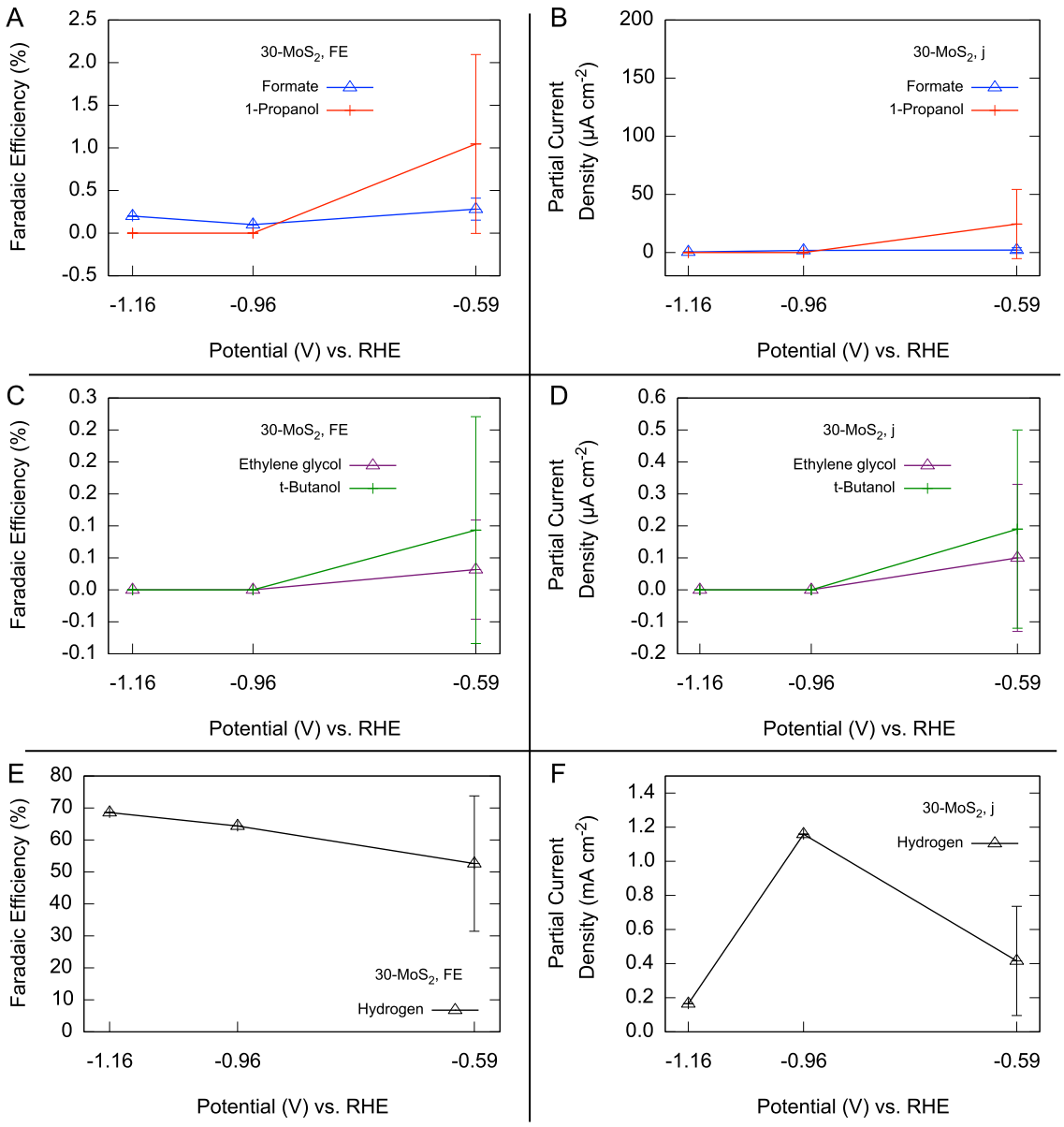

Figure S6. Potential-dependent Faradaic efficiencies (left) and partial current densities (right) for major (A,B), and minor CO_2R products (C,D), and proton reduction (E,F) on 30-MoS_2. The electrolyte was 0.10 M Na_2CO_3 (aq) acidified to pH 6.8 with 1 atm CO_2. Standard deviations are indicated for products at the least reducing potential evaluated.

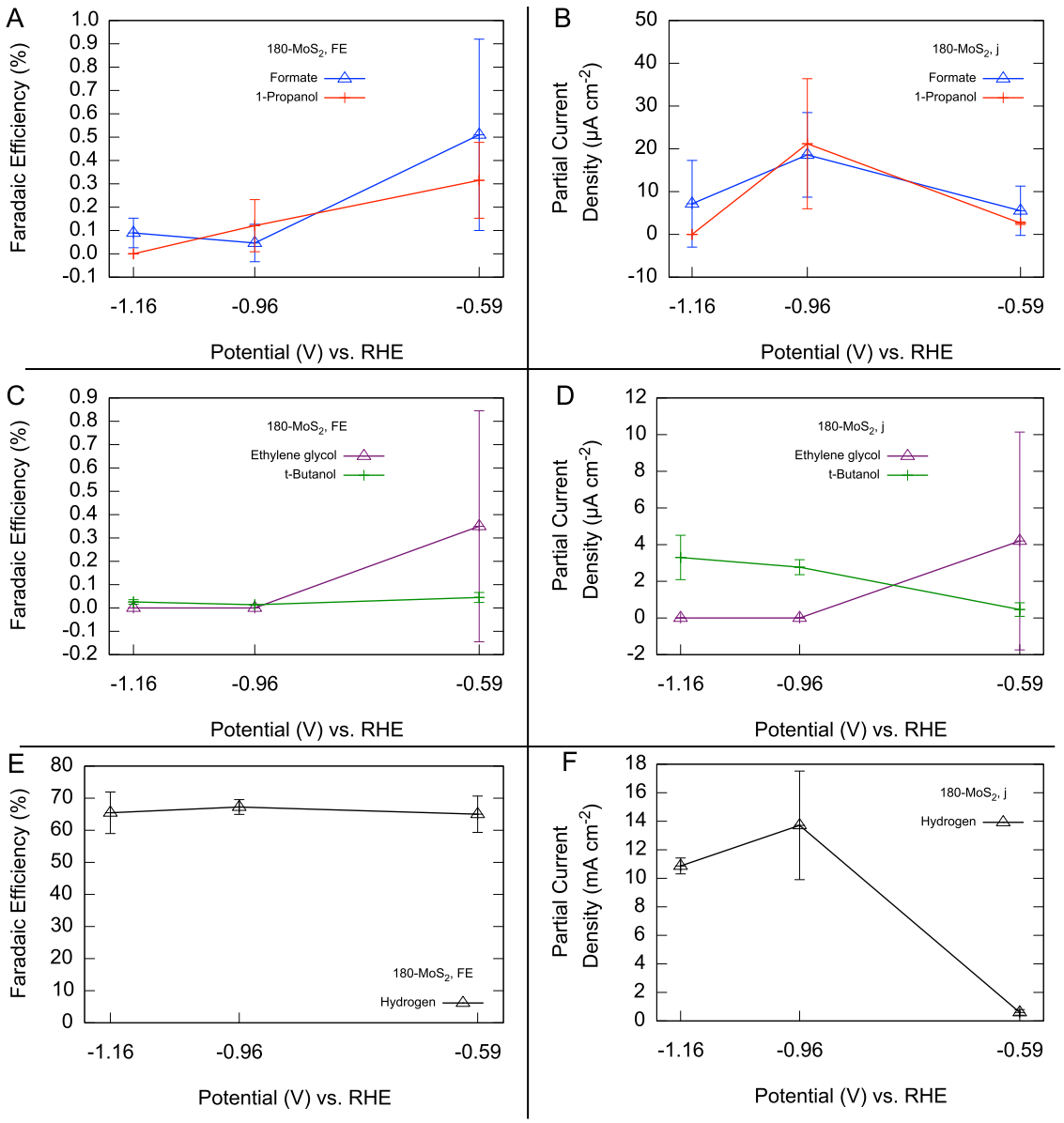

Figure S7. Potential-dependent Faradaic efficiencies (left) and partial current densities (right) for major (A,B), and minor CO_2R products (C,D), and proton reduction (E,F) on 180-MoS_2. The electrolyte was 0.10 M Na_2CO_3 (aq) acidified to pH 6.8 with 1 atm CO_2. Standard deviations are indicated for products.

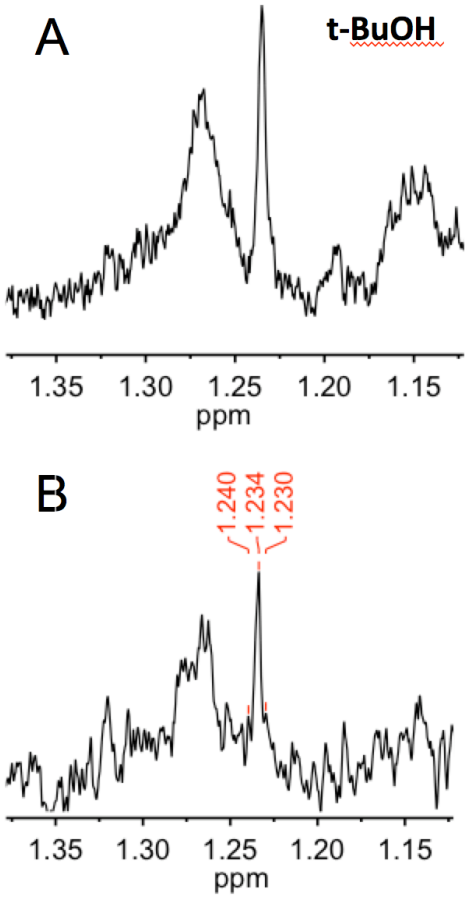

Figure S8. Representative NMR spectra in the 6H,s t-butanol region showing (A) t-butanol produced during unlabelled CO_2R on MoS_2 single crystal terraces, (B) labelled t-butanol production from $^{13}CO_2R$ on MoS_2 single crystal terraces. Electrolyses were performed at -0.59V vs. RHE in 0.1 M Na_2CO_3 electrolyte acidified to pH 6.8 with 1 atm of reactant gas.

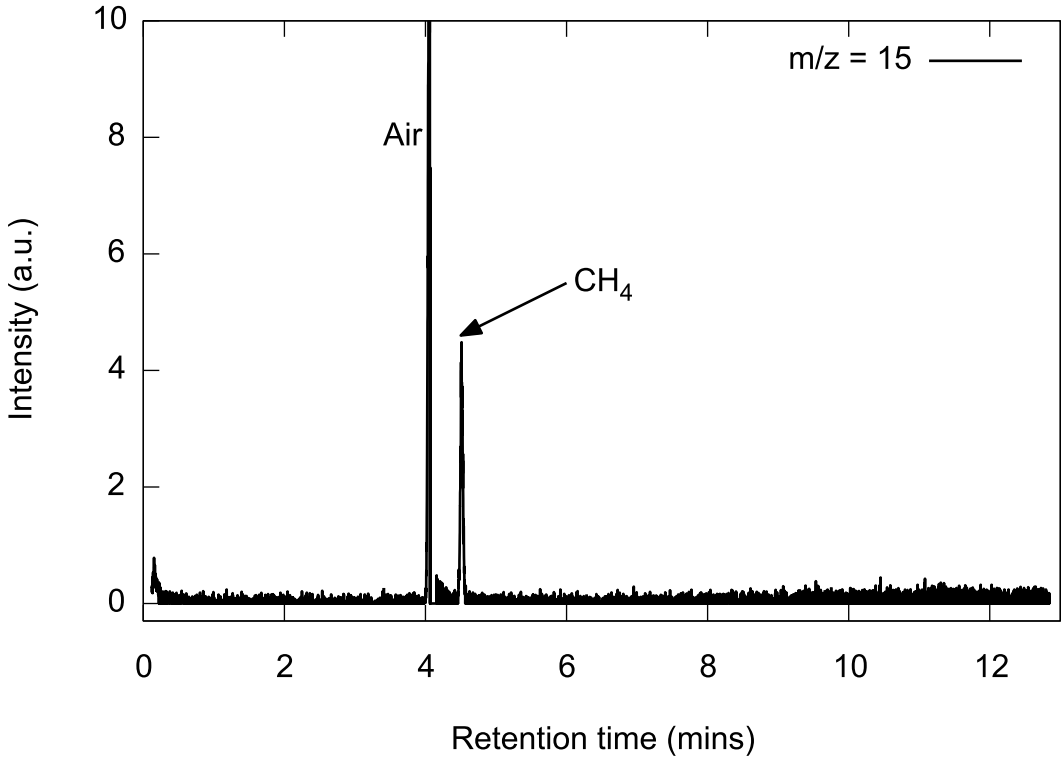

Figure S9. Representative chromatogram for the GC-MS analysis of gas products from CO reduction on a MoS_2 terrace. Electrolysis was performed at -0.59 V vs. RHE in 0.10 M K_2HPO_4 (aq) buffered to pH 6.8 with KH_2PO_4 (aq) and purged with CO(g). The total charge passed was 60 Coulombs.

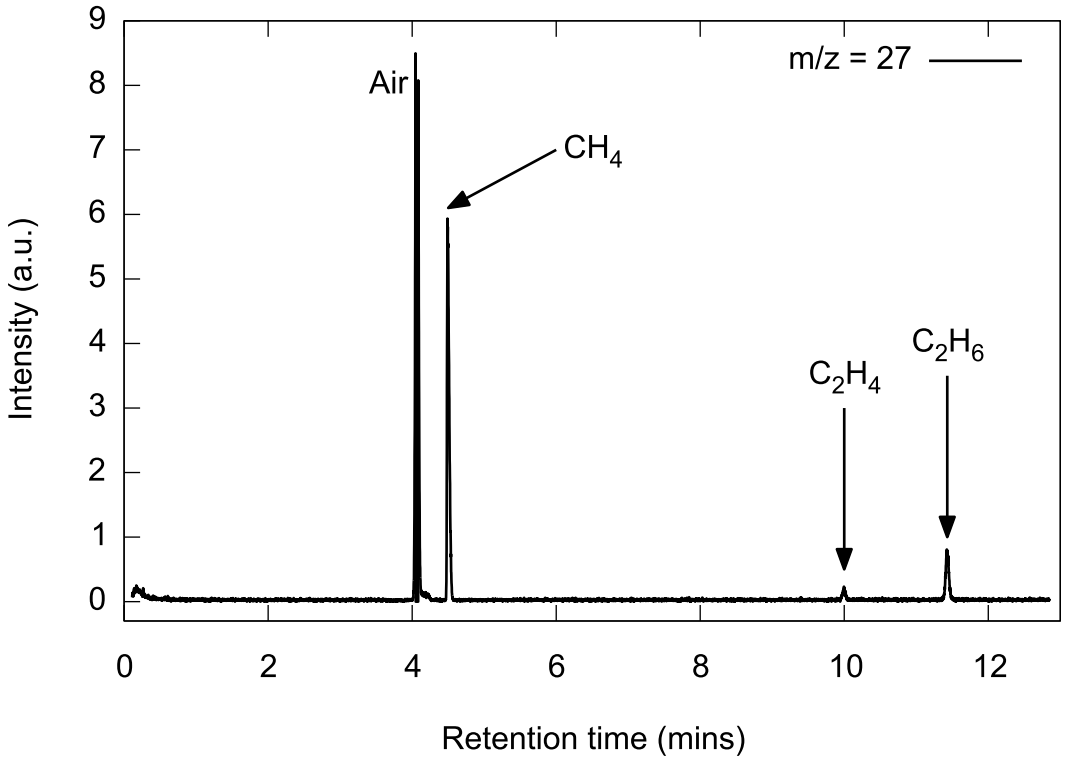

Figure S10. Representative chromatogram for the GC-MS analysis of gaseous products from CH_4 reduction on a MoS_2 terrace. Electrolysis was performed at -0.59 V vs. RHE in 0.10 M K_2HPO_4(aq) buffered to pH 6.8 with KH_2PO_4(aq) and purged with CH_4 gas. The total charge passed was 60 Coulombs.

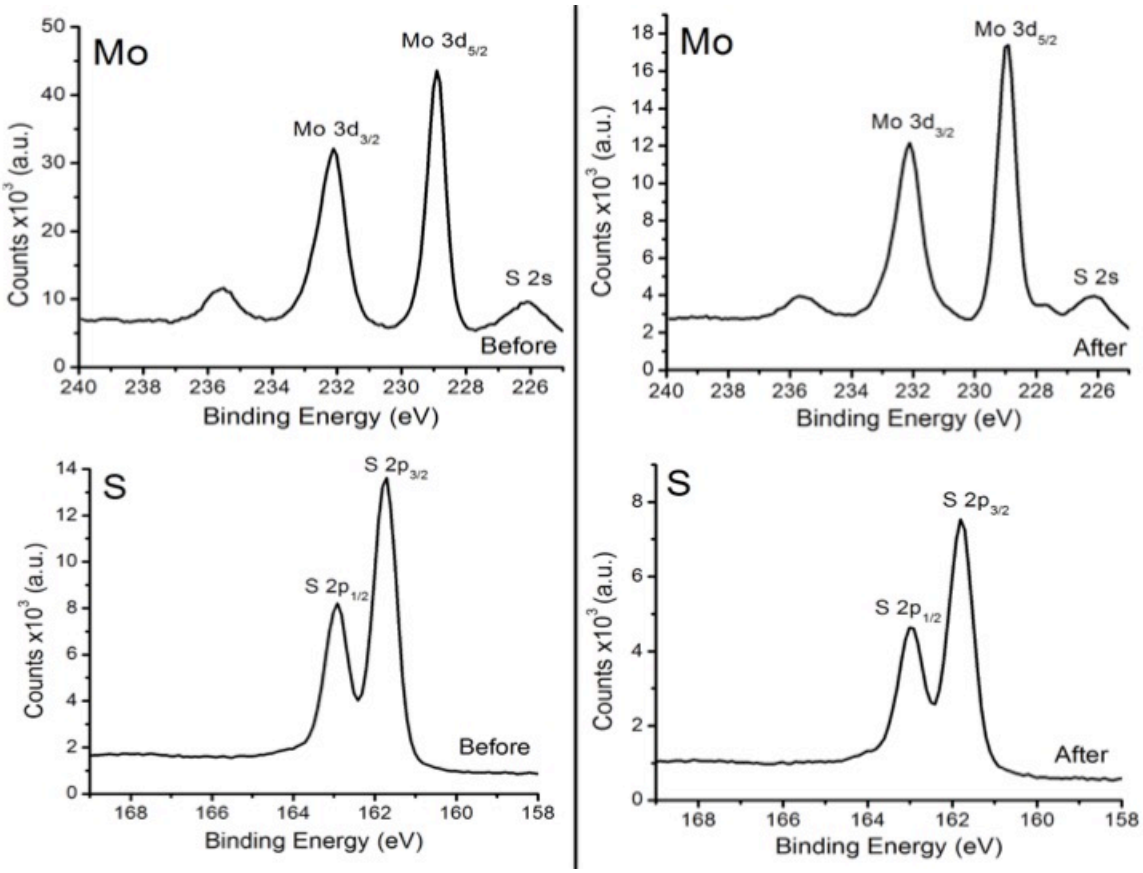

Figure S11. X-ray photoelectron spectroscopy of single crystals of MoS_2 before and after CO_2R, respectively**.**

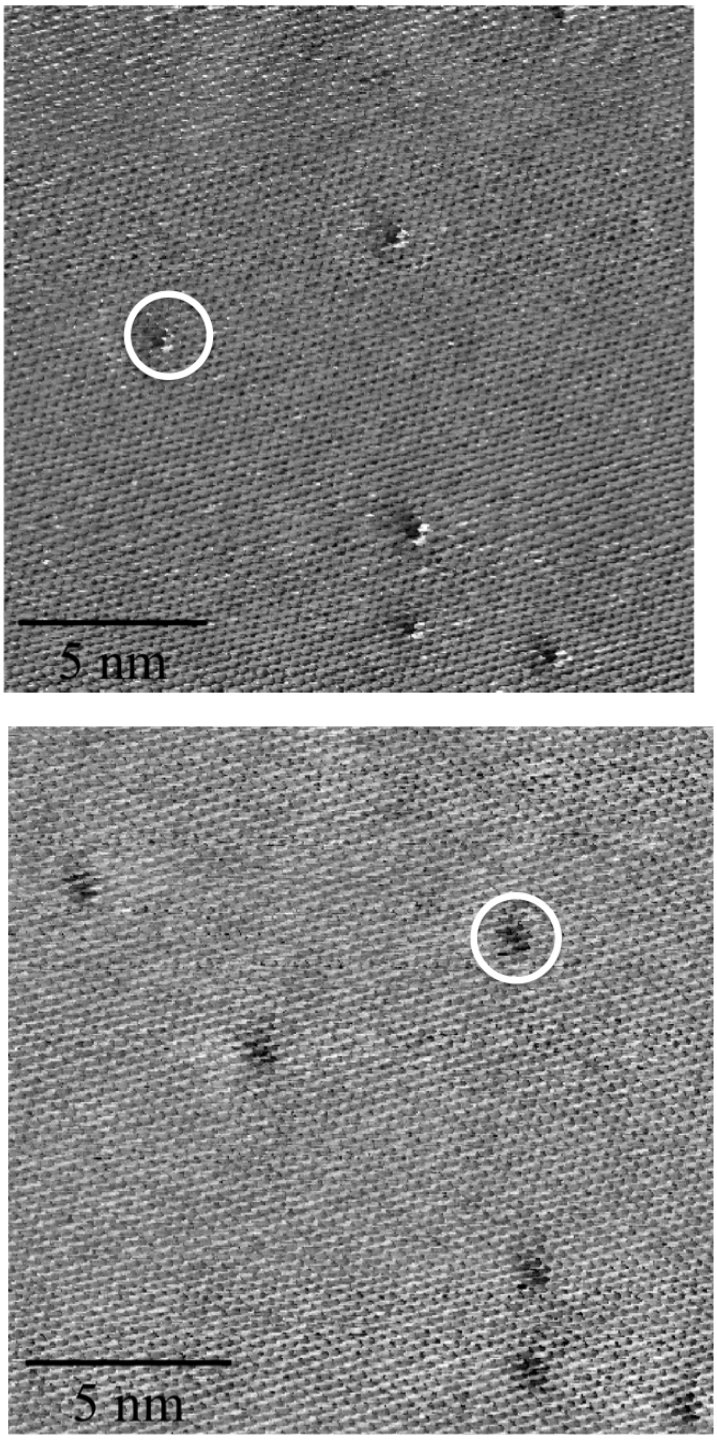

Figure S12. Scanning tunneling microscopy images showing sulfur vacancies on terraces of MoS_2 single crystals. The gap voltage was set to 1.3V, the tunneling current to 0.69 nA, the scan rate to 434 nm/s (forward scan direction (left to right)

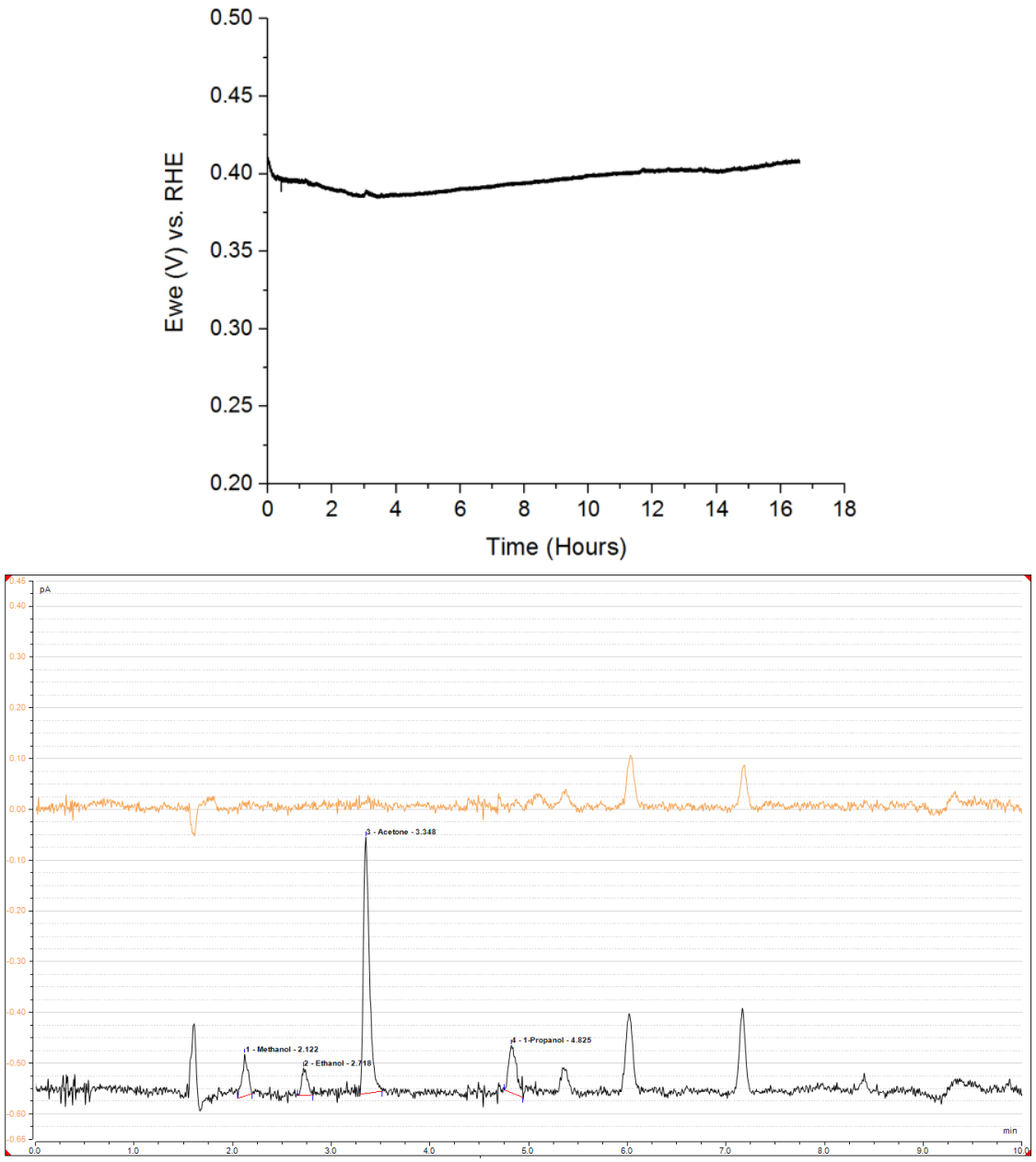

Figure S13. Open circuit voltages and GC-FID data for bulk single crystal MoS_2 in 0.1 M Na_2CO_3 solution purged with high purity CO_2 for one hour with no applied voltage. (A) Measured open circuit voltage vs. time. (B) . GC-FID data of two data sets. The orange chromatogram (top) shows a 16.5 hour run with background subtraction resulting in no prominent peaks of interest. The peaks at 6 and 7 minutes are caused by water vapor interacting with the column. The black chromatagram (bottom) shows 1 μM calibration solutions of methanol, ethanol, acetone, and 1-propanol. Chromatograms demonstrate that no key alcohol products derived from CO_2 reduction were formed when no current was being applied.

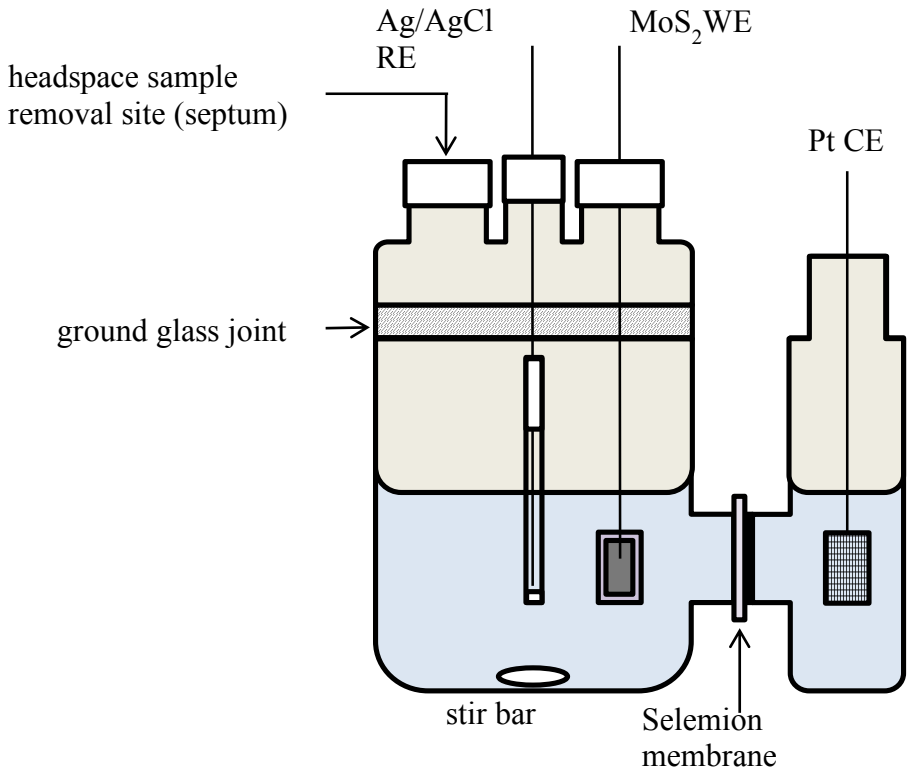

Figure S14. Schematic of the sealed custom H-cellused for the electrochemical experiments.

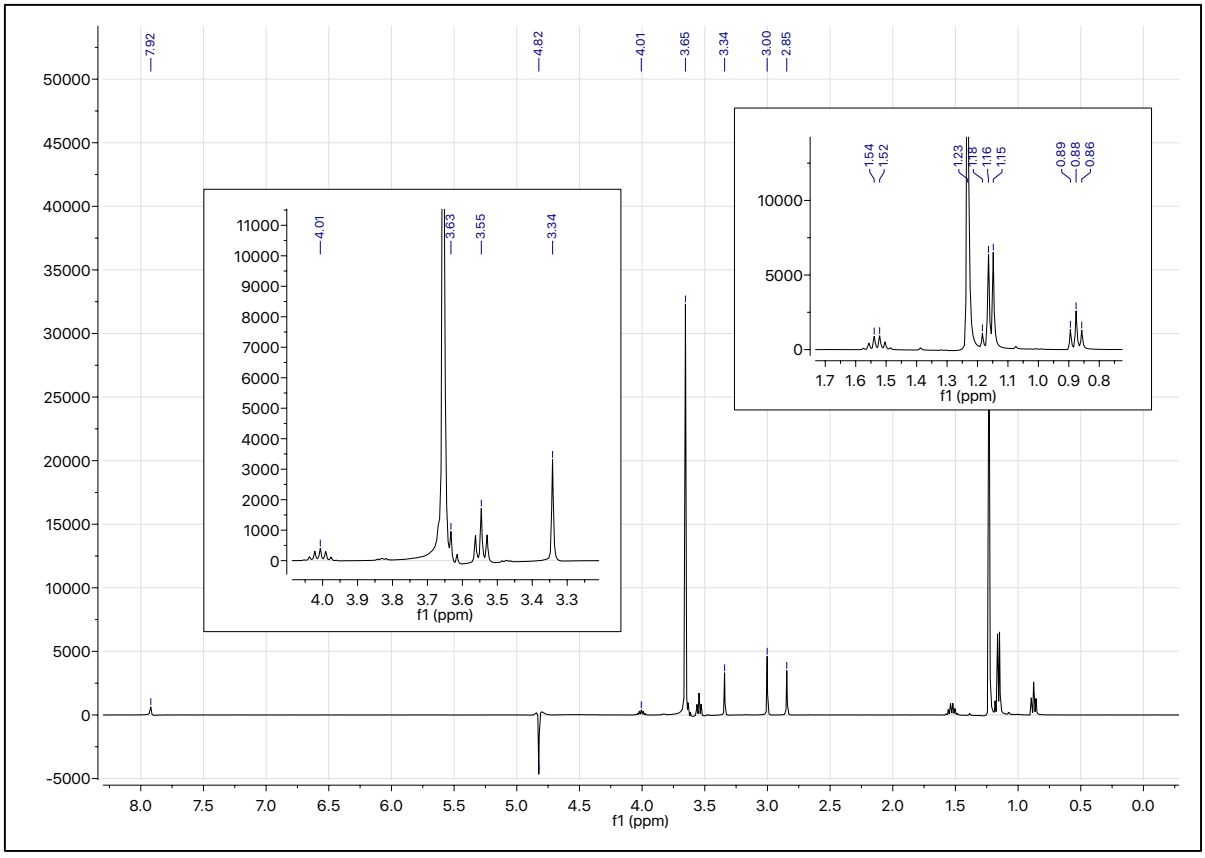

Figure S15. NMR spectrum showing chemical shifts of standards ~0.002 vol % in 0.10 M Na_2CO_3 (aq). Dimethyl formamide (DMF) was used as the internal standard, with the aldehydic proton signal at 7.92 ppm used to calibrate the chemical shift positions. Peak chemical shifts are identified in Table S1.

Standard name	Resonant ^{1}H (in bold)	Chemical shift, f1 (ppm)	Splitting
formate	**H**COO^-	8.44	1H,s
dimethylformamide[a]	$(CH_3)_2NC(O)H$	7.92	1H,s
	$(C\mathbf{H}_3)_2NC(O)H$	3.00	3H,s
	$(C\mathbf{H}_3)_2NC(O)H$	2.85	3H,s
2-propanol	$CH_3C\mathbf{H}(OH)CH_3$	4.01	1H,m
	$C\mathbf{H}_3CH(OH)C\mathbf{H}_3$	1.16	6H,d
ethylene glycol	$HOC\mathbf{H}_2C\mathbf{H}_2OH$	3.66	4H,s
ethanol	$CH_3C\mathbf{H}_2OH$	3.64	2H,q
	$C\mathbf{H}_3CH_2OH$	1.17	3H,t
1-propanol	$CH_3CH_2C\mathbf{H}_2OH$	3.55	2H,t
	$CH_3C\mathbf{H}_2CH_2OH$	1.53	2H,sex
	$C\mathbf{H}_3CH_2CH_2OH$	0.88	3H,t
methanol	$C\mathbf{H}_3OH$	3.34	3H,s
acetone	$C\mathbf{H}_3(O)C\mathbf{H}_3$	2.20	6H,s
acetate	$C\mathbf{H}_3COO^-$	1.90	3H,s
t-butanol[b]	$(C\mathbf{H}_3)_3COH$	1.23	6H,s
methane	$C\mathbf{H}_4$	0.16	4H,s

Table S1. Chemical shifts of NMR peaks used for analysis of products and reactants relevant to CO_2R observed in this work.[a] Internal standard; [b] At < 1μM t-butanol, a broad shoulder at 1.27 ppm was visible with the main singlet.